

Supporting Information

Facile Synthesis of Novel Elastomers with Tunable Dynamics for Toughness, Self-healing and Adhesion

Liang Chen¹, Tao Lin Sun^{2,3,4}, Kunpeng Cui⁵, Daniel R. King^{2,3}, Takayuki Kurokawa^{2,3}, Yoshiyuki Saruwatari⁶, Jian Ping Gong^{2,3,5,*}

¹*Graduate School of Life Science, Hokkaido University, N21W11, Kita-ku, Sapporo 001-0021, Japan*

²*Faculty of Advanced Life Science, Hokkaido University, N21W11, Kita-ku, Sapporo 001-0021, Japan*

³ *Soft Matter GI-CoRE, Hokkaido University, N21W11, Kita-ku, Sapporo, Japan*

⁴*South China Advanced Institute for Soft Matter Science and Technology, South China University of Technology, Guangzhou, 381st Wushan Road, Tianhe District, 510640, China*

⁵*Institute for Chemical Reaction Design and Discovery (WPI-ICReDD), Hokkaido University, N21W10, Kita-ku, Sapporo 001-0021, Japan*

⁶*Osaka Organic Chemical Industry Ltd., 1-7-20 Azuchi-machi, Chuo-ku, 541-0052 Osaka, Japan*

Corresponding author: gong@sci.hokudai.ac.jp

1. Characterization

Differential Scanning Calorimetry DSC measurements were performed using a TA instrument (DSC2500). The sample of 5~10 mg was placed in a non-hermitic pan, and an empty pan was used as a reference pan. The DSC experiment was performed in a heat-cool cycle, most of the samples were performed at this procedure (isothermal 120 °C, 5 min; 120 °C jump to -20 °C; -20 to 120 °C, 10 °C/min; isothermal 120 °C, 5 min; 120 to -20 °C, 10 °C/min; jump to 20 °C), wherein the thermal transitions for the heating cycle were recorded. The glass transition temperature (T_g) was determined by the inflection point of the heat capacity with temperature sweep.

Rheological test Rheological tests were performed using an ARES rheometer (advanced rheometric expansion system, Rheometric Scientific Inc.). Prior to the measurement, the disc-shaped samples with thicknesses of ~ 1.5 mm and diameters of ~ 15 mm were adhered to the parallel plates with a super glue. Rheological frequency sweep tests from 0.1 to 100 rad/s were performed with a shear strain of 0.1% in the parallel-plates geometry over a wide temperature range at a temperature interval of 8 °C. According to the principle of time-temperature superposition (TTS), master curves of storage modulus G' , loss modulus G'' , and loss factor $\tan\delta$ were constructed at a reference temperature of 24 °C using a time scale multiplicative horizontal shift factor a_T and modulus scale multiplicative vertical shift factor b_T . a_T follows a simple Arrhenius equation dependence on the temperature (**Figure S3, S6**), and b_T in most of copolymers is varied in 0.9 \sim 1.1, except for P(PEA-co-IBA) ($F = 0.3$), indicating small changes in polymer density at different temperatures.

Uniaxial tensile test Tensile stress-strain measurements were performed by a tensile tester (Instron 5965) with the standard JIS-K6251-7 size (gauge length 12 mm (L_0), width 2 mm (d), and thickness 1.5 mm (w)). The dog-bone shaped samples were cut using a cutter driven by an air-compressor. The sample was stretched at a deformation rate of 100 mm/min in air. Unless specified otherwise, the stress refers to the engineering stress, σ , defined as the tensile force divided by the cross-section area of the un-deformed sample. The strain, ε , is defined as the deformation length divided by the gauge length of the un-deformed sample. The elongation ratio, λ , is defined as the stretching length divided by the gauge length of the un-deformed sample. The initial strain rate, $\dot{\varepsilon}$, refers to the engineering strain rate, was estimated from the tensile velocity divided by the gauge length of the un-deformed sample. Except specified, the stretch velocity was 100 mm/min, which gives a strain rate 0.14 s⁻¹. The work of extension to fracture W_b was estimated from the area under the stress-strain curve.

Single-edge notch test The fracture behavior of samples was studied by single-edge notch test using a tensile tester (Instron 5965) with 100 N or 1000 N load cell. The notched and unnotched samples with the rectangular shape (length 40 mm (L), width 10

mm (d), thickness 1.5 mm (w)) that was cut by a laser cutter (Universal Laser systems, Inc ULR-60) were used to measure the fracture energy, Γ . For the notched sample, an initial notch width, c ($= 2$ mm), was cut through the side edge to center part of the sample. The test piece was clamped on two sides by clamps. The initial gauge length of the sample between the clamps for the notched and unnotched samples was ~ 20 mm. The upper clamp was pulled upward at a constant velocity of 100 mm/min, while the lower clamp was fixed. The force-elongation curves of notch and unnotched samples were recorded during the deformation. The onset of the crack propagation of notched sample was determined by a digital camera. The fracture energy was calculated from

the equation: $\Gamma = \frac{6W(\lambda_c)c}{\sqrt{\lambda_c}}$, where $W(\lambda_c)$ represents the strain energy density for unnotched sample at the elongation of λ_c , c is the initial notch width of notched sample, and λ_c is the critical elongation for onset of crack propagation of notched sample determined by the digital camera.

Stress distribution via optical polarizing observation To observe the stress distribution and neck-propagation during deformation, a homemade circular polarizing optical system was established with the tensile tester, according to the method described in our previous work [1]. A video camera and a white lamp were installed in front side and back side of tested sample, respectively. Two pieces of circular polarizer films were fixed, respectively, on the front of camera lens and lamp. The video camera was used to track the shape and isochromatic images of the sample upon stretching until the sample fractured. This simple method shows the stress distribution of the samples during deformation.

Lap-shear test The lap shear test was performed to quantify the adhesive behavior of elastomer on glass and polymethylmethacrylate (PMMA) which were used without further treatment. A piece of elastomer with cuboid geometry (1.5 cm \times 1.5 cm \times 1.5mm) was cut by a laser cutter (Universal Laser systems, Inc ULR-60). The two sides of the sample were brought into contact with the two solid

substrates by pressurized with a weight of 200g, which form a junction contact area of 2.25 cm². Then the ends of the solid substrates were clamped to the tensile machine. The upper clamp stretched the solid substrates at a shear rate of 10 mm min⁻¹ until the sample debonded from the substrates. The critical energy release rate, G_c was calculated as the expression [2]: $G_c = \left(\frac{F}{w}\right)^2 / (4Eh)$ where the F , E , h and w denote adhesive failure force, the elastic modulus, thickness, and width of sample, respectively.

2. Supplementary results

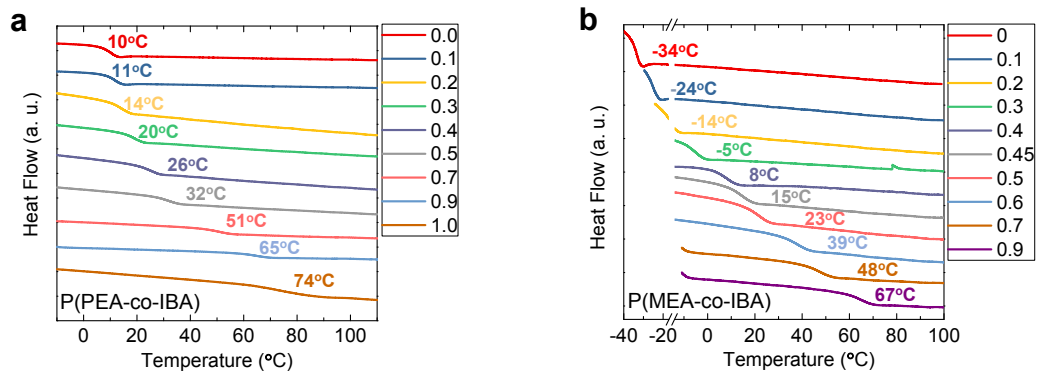


Figure S1. DSC curves of copolymers. (a) P(PEA-co-IBA) with various F ; (b) P(MEA-co-IBA) with various F . The numbers in the right columns of the figures are IBA molar fraction, F .

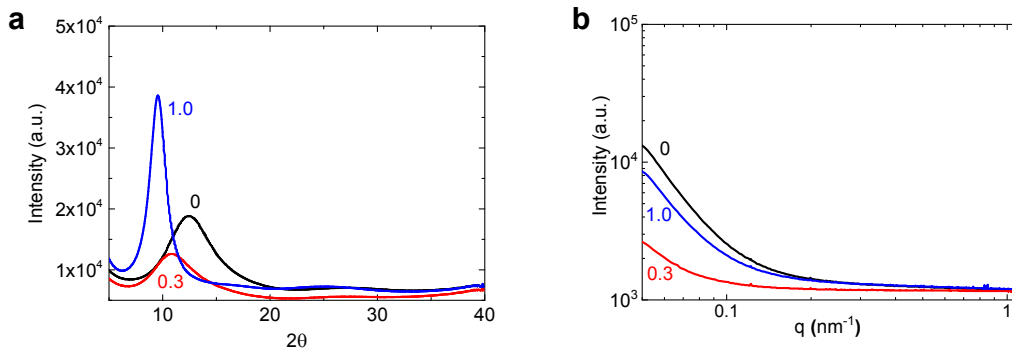


Figure S2. WAXS (a) and SAXS (b) profiles for PPEA ($F = 0$), P(PEA-co-IBA) ($F = 0.3$) and PIBA ($F = 1$), as representative samples. The numbers in the figure are IBA molar fraction, F .

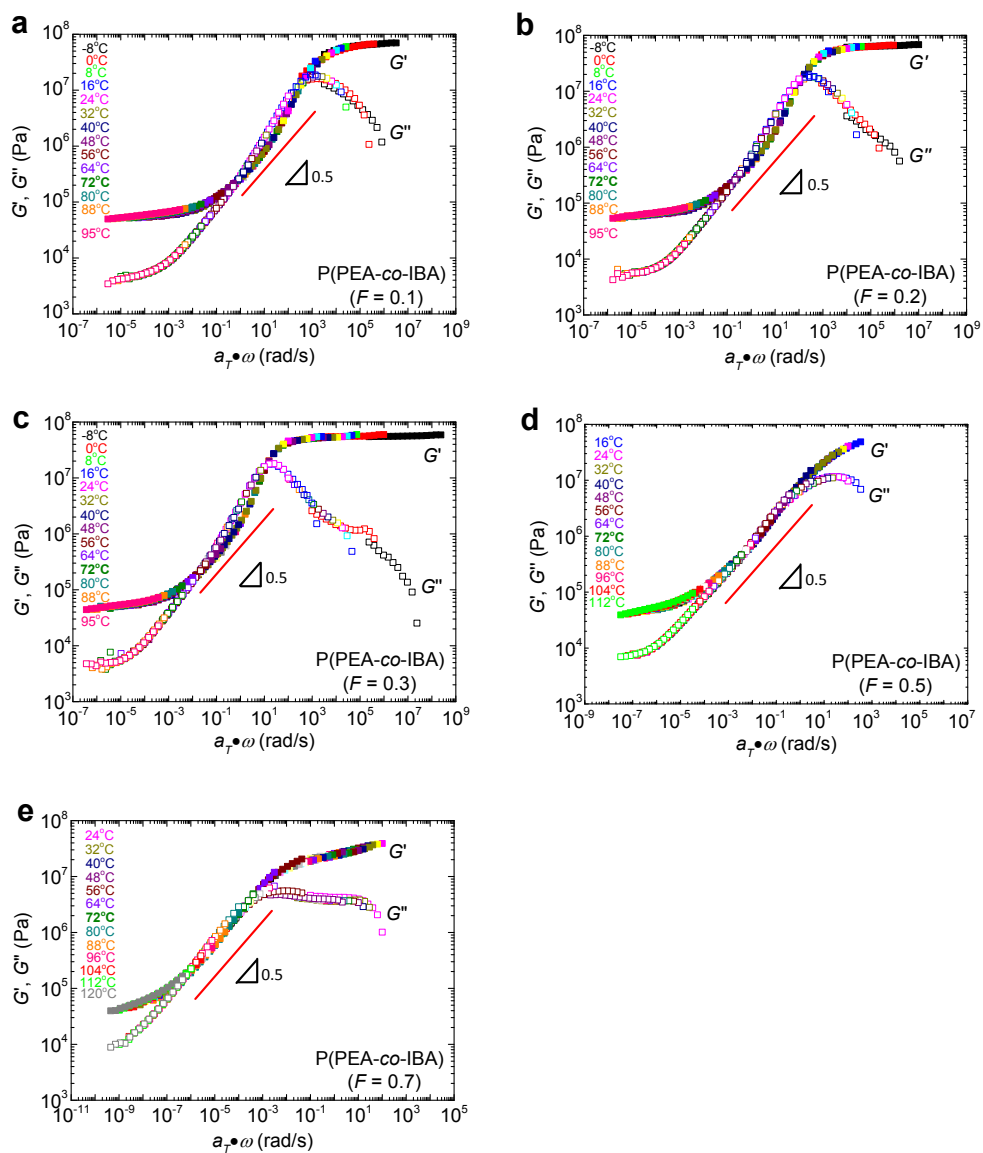


Figure S3. Master curves of G' and G'' of P(PEA-co-IBA) elastomers at different IBA fractions, F , at 24 °C. (a) $F = 0.1$; (b) $F = 0.2$; (c) $F = 0.3$; (d) $F = 0.5$; (e) $F = 0.7$. The solid lines in (a) - (e) have a slope of 0.5

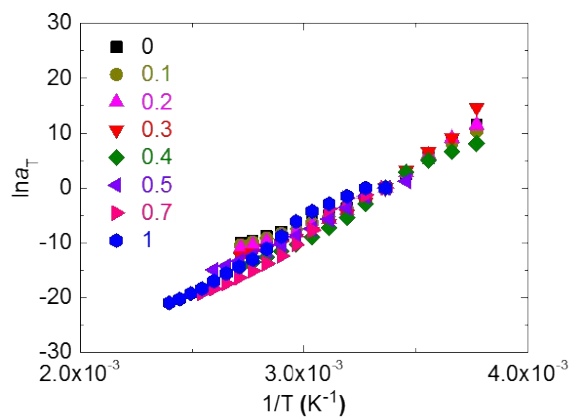


Figure S4. Temperature dependence of horizontal shift factors used to construct the master curves in **Figure 2** and **Figure S3** for P(PEA-co-IBA) elastomers. The numbers in the figure are IBA molar fraction, F .

Table S1. Characteristic relaxation times of the P(PEA-co-IBA) elastomers with varied IBA molar fraction, F , estimated from **Figure 2** and **Figure S3** using flexible linear polymer melt theory.

F	0	0.1	0.2	0.3	0.4	0.5	0.7	1
τ_0 (s)	$4.0 \cdot 10^{-4}$	$6.4 \cdot 10^{-4}$	$2.3 \cdot 10^{-3}$	$4.0 \cdot 10^{-2}$	$2.8 \cdot 10^{-1}$	$4.7 \cdot 10^{-1}$	$1.3 \cdot 10^2$	$3.8 \cdot 10^2$
τ_e (s)	$3.9 \cdot 10^{-1}$	$1.8 \cdot 10^0$	$4.3 \cdot 10^0$	$7.7 \cdot 10^1$	$5.0 \cdot 10^2$	$6.7 \cdot 10^2$	$1.6 \cdot 10^6$	$6.4 \cdot 10^6$
τ_p (s)	$1.1 \cdot 10^{-2}$	$2.6 \cdot 10^{-2}$	0.1	1.0	10.5	18.5	$3.9 \cdot 10^4$	$1.7 \cdot 10^5$

* τ_0 , τ_e are Kuhn segment relaxation time and the longest Rouse time of entangled strands, respectively, and τ_p is the inverse of frequency at which $\tan \delta = G''/G'$ shows a peak.

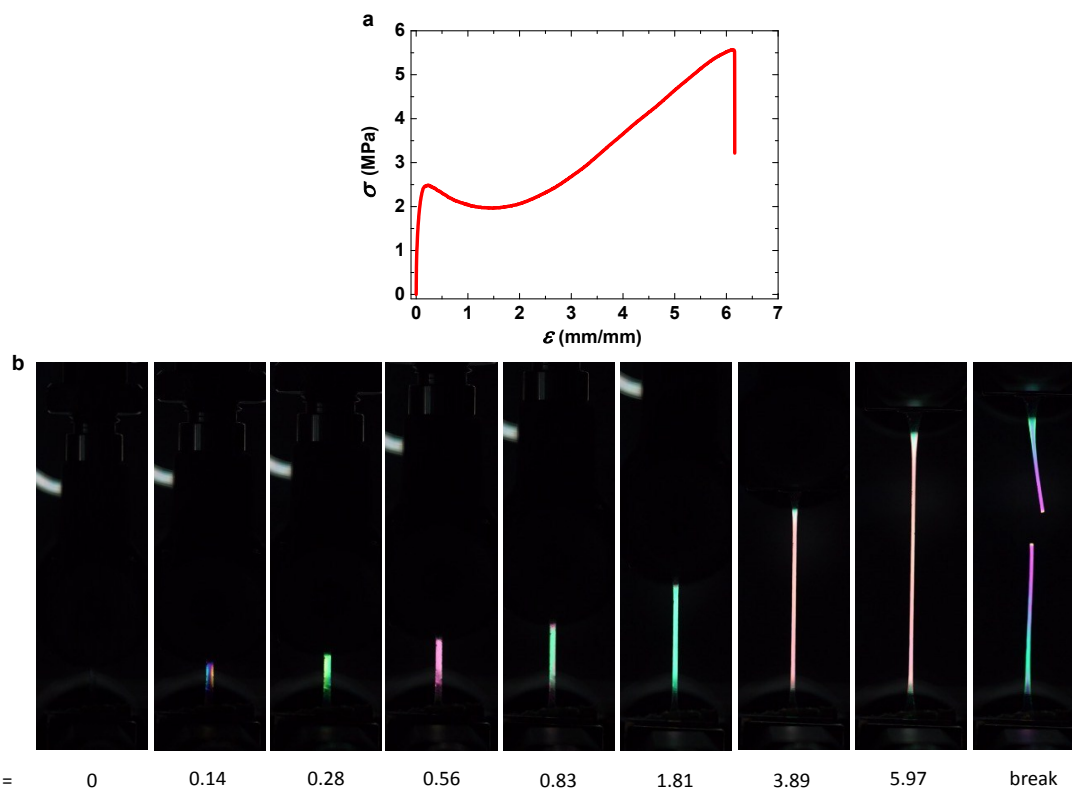


Figure S5. P(PEA-co-IBA) (0.3) was used to check stress distribution via polarizing optical (a) Stress-strain curves during stretching; (b) Optical images at different strains, ε , when subjected to uniaxial tensile test.

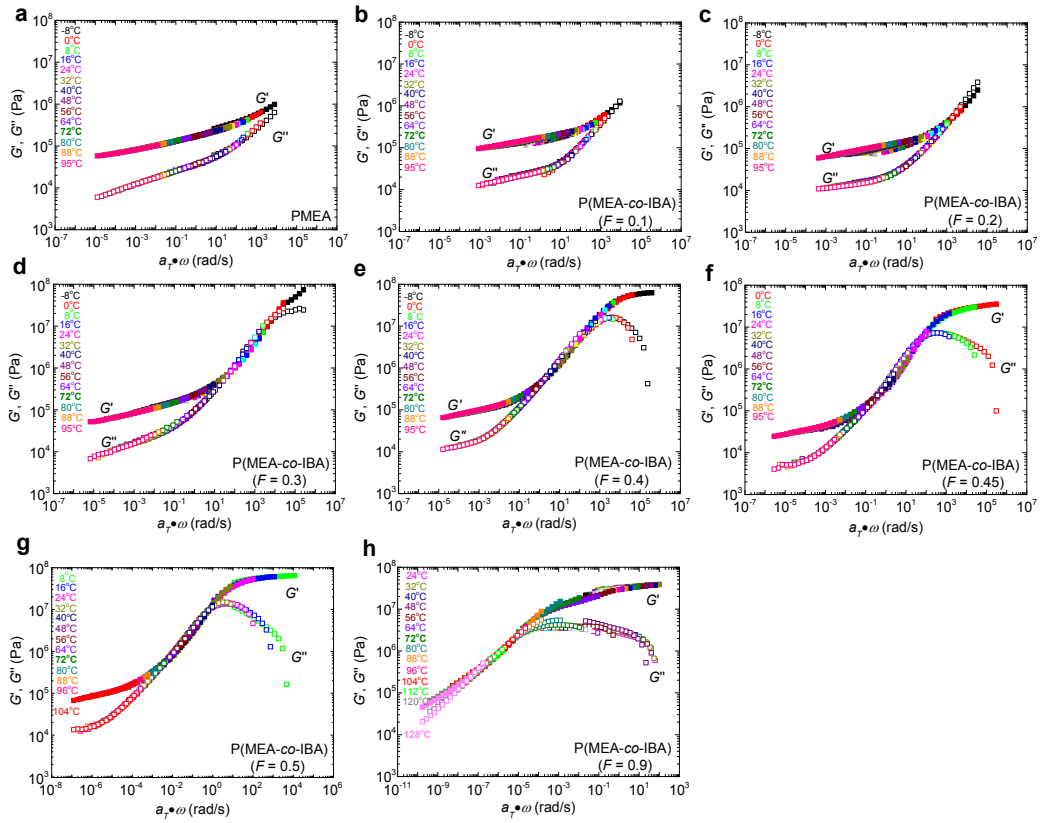


Figure S6. Master curves of G' and G'' of P(MEA-co-IBA) elastomers at different IBA fractions, F , at 24 °C.

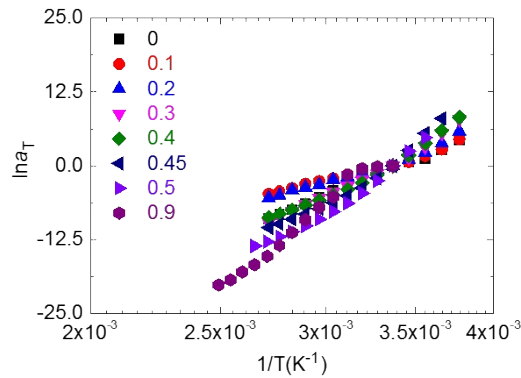


Figure S7. Temperature dependence of horizontal shift factors used to construct the master curves in Figure S6. The numbers in the figure are IBA molar fraction, F .

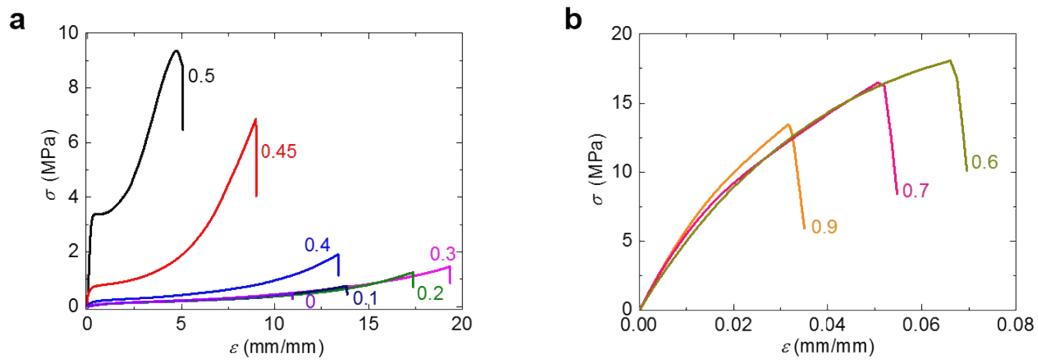


Figure S8. Stress-strain curves of P(MEA-co-IBA) elastomers at 24 °C with a strain rate 0.14 s⁻¹. The numbers in the figures are IBA molar fraction, F . (a) Samples with F from 0 to 0.5; (b) Samples with F above 0.6.

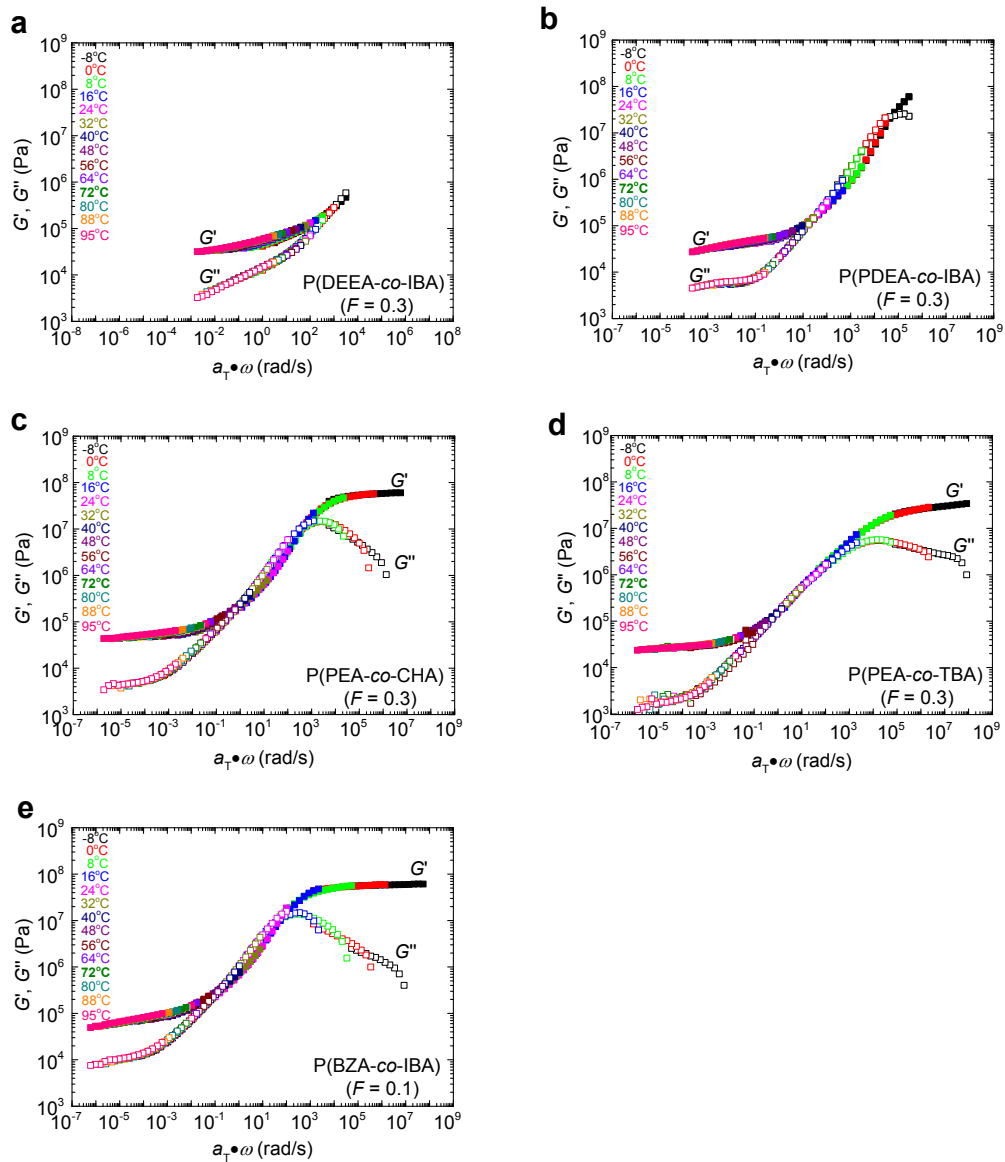


Figure S9. Master curves of G' and G'' of elastomers from various copolymers at 24 °C. F is the molar fraction of high T_g monomer.

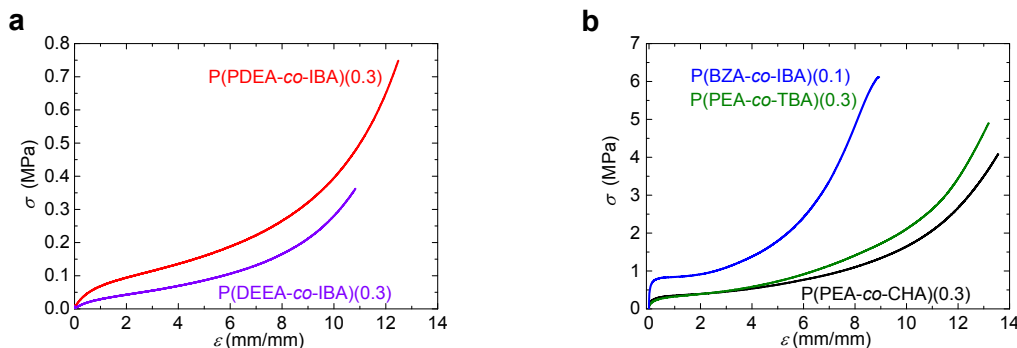


Figure S10. Stress-strain curves of copolymers at 24 °C with a strain rate 0.14 s⁻¹. (a) P(DEEA-co-IBA) ($F = 0.3$) and P(PDEA-co-IBA) ($F = 0.3$); (b) P(PEA-co-CHA) ($F = 0.3$), P(PEA-co-TBA) ($F = 0.3$), and P(BZA-co-IBA) ($F = 0.1$). F is the molar fraction of high T_g monomer.

Table S2. Mechanical behaviors of elastomers using different monomer combinations.

Sample Code	τ_0 (s)	T_g (°C)	E (MPa)	σ_b (MPa)	ϵ_b (mm/mm)	W_{ext} (MJ/m ³)	Γ (kJ/m ²)	η_e (%)
P(DEEA-co-IBA) (0.3)	-----	-34	0.042 ± 0.0014	0.25 ± 0.014	9.43 ± 0.33	0.87 ± 0.042	0.53 ± 0.01	33.16 ± 7.85
P(PDEA-co-IBA) (0.3)	6.6*10 ⁻⁶	-4	0.12 ± 0.024	0.71 ± 0.06	12.11 ± 0.36	2.97 ± 0.13	0.86 ± 0.13	69.55 ± 24.19
P(PEA-co-CHA) (0.3)	4.4*10 ⁻⁴	12	0.73 ± 0.23	3.96 ± 0.36	13.73 ± 0.32	6.12 ± 1.68	4.72 ± 0.29	62.32 ± 7.40
P(PEA-co-TBA) (0.3)	1.0*10 ⁻⁴	13	0.85 ± 0.014	4.72 ± 0.23	12.83 ± 0.47	18.72 ± 0.54	6.02 ± 0.35	56.30 ± 2.59
P(BZA-co-IBA) (0.1)	3.3*10 ⁻³	18	2.81 ± 0.68	6.62 ± 0.74	10.11 ± 1.07	22.42 ± 4.99	10.84 ± 0.71	37.00 ± 4.91

1) Samples are coded as P(A-co-B) (F), where A and B are the name of monomers with low T_g and high T_g of their homopolymers, respectively, and F indicates the molar fraction of high T_g monomer in the copolymer. The error ranges are the standard deviation from at least three samples.

2) Strain rate is 0.14 s⁻¹ for tensile test and 0.083 s⁻¹ for single-edge notch test.

3) Dashes indicate that the Kuhn monomer relaxation time τ_0 of P(DEEA-co-IBA) (0.3) is too short to be observed.

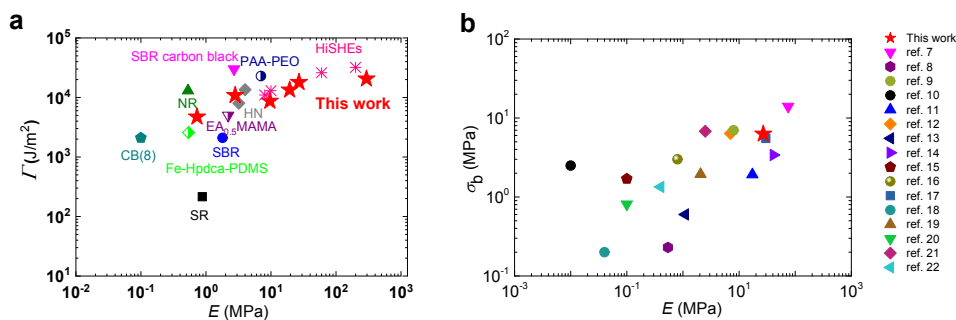


Figure S11. (a) Ashby plot of toughness versus Young's modulus of our elastomers and other polymeric elastomers reported in related references. SR: silicon rubber [3]; NR: Natural Rubber; SBR: Styrene-Butadiene Rubber [4,5]; SBR Carbon black [5]; EA_{0.5}MAMA: Triple network elastomer [6]; HN: Hybrid networks [7]; Fe-Hpdca-PDMS: poly(dimethylsiloxane) polymer chains crosslinked by coordination complexes [8]; HiSHEs: polyampholyte-based elastomer [9]. (b) Ashby plot of fracture stress versus Young's modulus of our elastomers and other room temperature self-healing elastomers reported in recented literatures. The plots show that our elastomers showed in red star by random copolymerization have strength/toughness comparable with that of previous reports.

References

- [1] F. Luo, T. L. Sun, T. Nakajima, T. Kurokawa, Y. Zhao, A. B. Ihsan, H. L. Guo, X. F. Li, J. P. Gong, *Macromolecules*, **2014**, *47*, 6037.
- [2] C. K. Roy, H. L. Guo, T. L. Sun, A. B. Ihsan, T. Kurokawa, M. Takahata, T. Nonoyama, T. Nakajima, J. P. Gong, *Adv. Mat.* **2015**, *27*, 7344.
- [3] C. Wang, C.-I. Chang, *J. Appl. Polym. Sci.* **2000**, *75*, 1033.
- [4] A. N. Gent, S.-M. Lai, C. Nah, C. Wang, *Rubb. Chem. Technol.* **1994**, *67*, 610.
- [5] A. Ahagon, A. N. Gent, H. J. Kim, Y. Kumagai, *Rubb. Chem. Technol.* **1975**, *48*, 896.
- [6] E. Ducrot, Y. Chen, M. Bulters, R. P. Sijbesma, C. Creton, *Science* **2014**, *344*, 186.
- [7] J. Wu, L. H. Cai, D. A. Weitz, *Adv. Mater.* **2017**, *29*, 1702616.
- [8] C.-H. Li, C. Wang, C. Keplinger, J. Zuo, L. Jin, Y. Sun, P. Zheng, Y. Cao, F. Lissel, C. Linder, X.-Z. You, Z. Bao, *Nat. Chem.* **2016**, *8*, 618.
- [9] Y. Peng, L. Zhao, C. Yang, Y. Yang, C. Song, Q. Wu, G. Huang, J. Wu, *J. Mater. Chem. A* **2018**, *6*, 19066
- [10] P. Cordier, F. Tournilhac, C. Soulié-Ziakovic, L. Leibler, *Nature* **2008**, *451*, 977.
- [11] Y. Chen, A. M. Kushner, G. A. Williams, Z. Guan, *Nat. Chem.* **2012**, *4*, 467.
- [12] Y. Wang, X. Liu, S. Li, T. Li, Y. Song, Z. Li, W. Zhang, J. Sun, *ACS Appl. Mater. Interfaces* **2017**, *9*, 29120.
- [13] Y.-L. Rao, A. Chortos, R. Pfattner, F. Lissel, Y. C. Chiu, V. Feig, J. Xu, T. Kurosawa, X. Gu, C. Wang, M. He, J. W. Chung, Z. Bao, *J. Am. Chem. Soc.* **2016**, *138*, 6020.
- [14] D. Mozhdzhi, S. Ayala, O. R. Cromwell, Z. Guan, *J. Am. Chem. Soc.* **2014**, *136*, 16128.
- [15] J. Liu, C. S. Y. Tan, Z. Yu, N. Li, C. Abell, O. A. Scherman, *Adv. Mater.* **2017**, *29*, 1605325.
- [16] Y. Miwa, J. Kurachi, Y. Kohbara, S. Kutsumizu, *Commun. Chem.* **2018**, *1*, 5.

- [17] A. Susa, R. K. Bose, A. M. Grande, S. van der Zwaag, S. J. Garcia, *ACS Appl. Mater. Interfaces* **2016**, *8*, 34068.
- [18] P.-F. Cao, B. Li, T. Hong, J. Townsend, Z. Qiang, K. Xing, K. D. Vogiatzis, Y. Wang, J. W. Mays, A. P. Sokolov, T. Saito, *Adv. Funct. Mater.* **2018**, *28*, 1800741.
- [19] Y. Chen, Z. Tang, X. Zhang, Y. Liu, S. Wu, B. Guo, *ACS Appl. Mater. Interfaces* **2018**, *10*, 24224.
- [20] A. Rekondo, R. Martin, A. R. Luzuriaga, G. Cabañero, H. J. Grande, I. Odriozola, *Mater. Horiz.* **2014**, *1*, 237.
- [21] Q. Zhang, S. Niu, L. Wang, J. Lopez, S. Chen, Y. Cai, R. Du, Y. Liu, J.-C. Lai, L. Liu, C.-H. Li, X. Yan, C. Liu, J. B.-H. Tok, X. Jia, Z. Bao, *Adv. Mater.* **2018**, *30*, 1801435.
- [22] L. Zhang, Z. Liu, X. Wu, Q. Guan, S. Chen, L. Sun, Y. Guo, S. Wang, J. Song, E. M. Jeffries, C. He, F.-L. Qing, X. Bao, Z. You. *Adv. Mater.* **2019**, 1901402.

Supplementary Movie S1

A movie showing single-edge notch test to measure the fracture energy of elastomer of (PEA-co-IBA) ($F = 0.3$) at the strain rate of 0.083 s^{-1} .

Supplementary Movie S2

A movie showing the self-healing properties of P(PEA-co-IBA) ($F = 0.3$) at 24°C .

Supplementary Movie S3

A movie showing the comparison of toughness between a P(PEA-co-IBA) ($F = 0.3$) sample and a natural rubber.